Peter N. Jordan and David J. Christini
Am J Physiol Heart Circ Physiol 293:2109-2118, 2007. First published Jun 22, 2007;
doi:10.1152/ajpheart.00609.2007

You might find this additional information useful...

This article cites 24 articles, 8 of which you can access free at:
http://ajpheart.physiology.org/cgi/content/full/293/4/H2109#BIBL

Updated information and services including high-resolution figures, can be found at:
http://ajpheart.physiology.org/cgi/content/full/293/4/H2109

Additional material and information about ***AJP - Heart and Circulatory Physiology*** can be found at:
http://www.the-aps.org/publications/ajpheart

This information is current as of October 9, 2007 .

AJP - Heart and Circulatory Physiology publishes original investigations on the physiology of the heart, blood vessels, and lymphatics, including experimental and theoretical studies of cardiovascular function at all levels of organization ranging from the intact animal to the cellular, subcellular, and molecular levels. It is published 12 times a year (monthly) by the American Physiological Society, 9650 Rockville Pike, Bethesda MD 20814-3991. Copyright © 2005 by the American Physiological Society. ISSN: 0363-6135, ESSN: 1522-1539. Visit our website at http://www.the-aps.org/.

Downloaded from ajpheart.physiology.org on October 9, 2007

Am J Physiol Heart Circ Physiol 293: H2109–H2118, 2007.
First published June 22, 2007; doi:10.1152/ajpheart.00609.2007.

Characterizing the contribution of voltage- and calcium-dependent coupling to action potential stability: implications for repolarization alternans

Peter N. Jordan[1] and David J. Christini[1,2]

[1]*Department of Physiology and Biophysics, Weill Graduate School of Medical Sciences of Cornell University, and* [2]*Division of Cardiology, Department of Medicine, Weill Cornell Medical College, New York, New York*

Submitted 24 May 2007; accepted in final form 22 June 2007

Jordan PN, Christini DJ. Characterizing the contribution of voltage- and calcium-dependent coupling to action potential stability: implications for repolarization alternans. *Am J Physiol Heart Circ Physiol* 293: H2109–H2118, 2007. First published June 22, 2007; doi:10.1152/ajpheart.00609.2007.—Experiments have provided suggestive but inconclusive insights into the relative contributions of transmembrane voltage and intracellular calcium handling to the development of cardiac electrical instabilities such as repolarization alternans. In this study, we applied a novel combination of techniques (action potential voltage clamping, calcium-transient clamping, and stability analysis) to cardiac cell models to more clearly determine the roles that voltage- and calcium-dependent coupling play in regulating action potential stability and the development of alternans subsequent to the loss of stability. Using these techniques, we are able to demonstrate that voltage- and calcium-dependent coupling exhibit varying degrees of influence on action potential stability across models. Our results indicate that cellular dynamic instabilities such as alternans may be initiated by either voltage- or calcium-dependent mechanisms or by some combination of the two. Based on these modeling results, we propose novel single-cell experiments that incorporate action-potential voltage clamping, calcium imaging, and real-time measurement of action potential stability. These experiments will make it possible to experimentally determine the relative contribution of voltage coupling to the regulation of action potential stability in real cardiac myocytes, thereby providing further insights into the mechanism of alternans.

calcium handling; ionic model

THE MECHANISM UNDERLYING REPOLARIZATION alternans, which occurs when the normal, nonalternating action potential morphology loses stability and bifurcates into a beat-to-beat alternation, in cardiac myocytes remains unclear, with the interdependence of transmembrane voltage and intracellular calcium cycling presenting "a difficult chicken and egg problem that remains unresolved" (23). At least two different mechanisms for alternans have been proposed: *1*) intracellular calcium cycling alternans causes repolarization alternans via some calcium-dependent sarcolemmal current(s), and *2*) repolarization alternans causes intracellular calcium alternans (23).

Insight into which (if not both) of these mechanisms operates in real cells has purportedly been obtained from AP voltage-clamp experiments on ventricular myocytes isolated from rabbits (2) and guinea pigs (25) and from conventional voltage-clamp experiments on myocytes isolated from cats (12). These experiments demonstrated that the intracellular calcium transient can alternate during AP or voltage clamping, i.e., in the absence of repolarization alternans. Although the mechanism underlying calcium alternans may be species specific, the results from these experiments demonstrate that beat-to-beat alternation of the intracellular calcium transient during AP clamping is an inherent property of the intracellular calcium dynamics of these cells and is not secondary to repolarization alternans (2).

These results seem to suggest that the governing factor for alternans in paced cells is the alternation of intracellular calcium, (i.e., *mechanism 1* mentioned above). The argument underlying such a contention is that the finding that intracellular calcium alternates when voltage is clamped means that calcium alternans must drive repolarization alternans when voltage is not clamped. Implicit in this argument is the assumption that clamping voltage does not interfere with the dominant mechanism of alternans in the cell; that is, such conclusions assume that the stability properties of AP-clamped and paced cells are essentially the same.

In this simulation study, we sought to determine whether this assumption is valid. If the cellular rhythm possesses the same stability properties during AP clamping as during pacing, it can be concluded that the same mechanism drives the behavior in both contexts. However, if the stability properties of the cellular rhythm change when voltage is clamped, this implies that the intracellular calcium handling system is not the only contributor to the stability properties of the rhythm. Furthermore, this would suggest that drawing conclusions about the behavior of paced cells based on the behavior of voltage-clamped cells is less straightforward than has previously been believed.

We demonstrate that a systematic study of the behavior of clamped and unclamped simulated cardiac cells, using a novel combination of techniques, can be used to quantify the stability of the cellular rhythm as it relates to the initiation of alternans. Our methodology indirectly reveals the contributions of various ionic components of the cell to modulating the stability of the cellular rhythm and hence reveals their roles in the development of instabilities leading to alternans. Based on these simulations, we propose new experiments to explore the roles of various ionic components of the cell in modulating the stability of the cellular rhythm in real cardiac myocytes.

CONCEPTUAL BASIS OF PROPOSED METHODOLOGY

Alternans arises when the cellular period-1 rhythm (i.e., identical morphologies of voltage, intracellular calcium concentration, etc., during consecutive beats) transitions from being stable to being unstable and is replaced by a stable

Address for reprint requests and other correspondence: D. J. Christini, Div. of Cardiology, Weill Cornell Medical College, 1300 York Ave., Box 161, New York, NY 10021 (e-mail: dchristi@med.cornell.edu).

The costs of publication of this article were defrayed in part by the payment of page charges. The article must therefore be hereby marked "*advertisement*" in accordance with 18 U.S.C. Section 1734 solely to indicate this fact.

 0363-6135/07 $8.00 Copyright © 2007 the American Physiological Society

Downloaded from ajpheart.physiology.org on October 9, 2007

period-2 (i.e., alternating) rhythm. Through analysis of the stability of the period-1 rhythm, we assess the roles of various cellular components in causing this transition to occur.

The method involves an analysis of the stability of the period-1 rhythm under three different conditions: *1*) during pacing, *2*) during AP-voltage clamping, and *3*) during calcium-transient clamping (a method only applicable in mathematical modeling, as in *Intracellular coupling during calcium-transient clamping*). The ability of our technique to extract pertinent information about the contributions of different components of the cell to alternans can be understood by considering the nature of the intracellular coupling that is present in each of these conditions.

Intracellular coupling during pacing. Figure 1 illustrates the nature of the intracellular coupling that governs the electrophysiology of cardiac myocytes. In a paced cell, voltage is bidirectionally coupled to all of the voltage-dependent sarcolemmal currents; that is, voltage and the voltage-dependent sarcolemmal currents mutually influence each other. Similarly, the intracellular calcium system is bidirectionally coupled to the calcium-dependent components (i.e., the calcium-dependent sarcolemmal currents and intracellular concentrations and fluxes) of the cell during pacing. In addition to those components that are solely voltage or calcium dependent, some electrophysiological components of the cell are both voltage and calcium dependent [e.g., L-type calcium current ($I_{Ca,L}$) and sodium-calcium exchanger current (I_{NaCa}) in Fig. 1]. The presence of this last set of components means that every ionic current, flux, ionic concentration, etc., within the cell indirectly interacts with and is influenced by the behavior of every other electrophysiological component of the cell during pacing, since pathways exist that couple every component of the cell to every other component of the cell.

It should be noted that the precise composition of the two groups of ionic currents shown in Fig. 1, those that are purely voltage dependent and those that are both voltage and calcium dependent, is dependent on the particular currents that are present in any given (real or model) cell. Although some currents (e.g., $I_{Ca,L}$) possess strong voltage and calcium dependence, other currents [e.g., a slow component of the delayed rectifier potassium current (I_{Ks})] appear to be more strongly voltage dependent than calcium dependent (16) and thus can be thought of as part of the purely voltage-dependent group of currents.

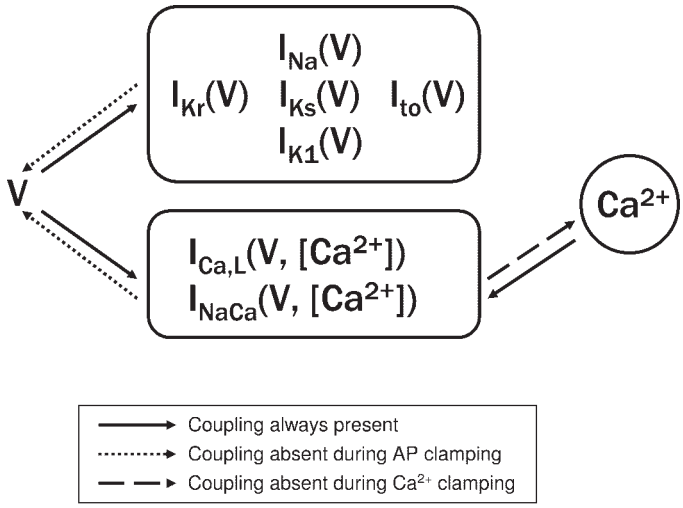

Fig. 1. Schematic representation of the coupling between cellular components. The voltage (V)-sensitive ionic currents shown here are those included in the Shiferaw et al (Ref. 19) modification of the canine ventricular myocyte (CVM) model; the components of the calcium system that are not sensitive to voltage are grouped together (as depicted by the "Ca^{2+}" enclosed in the circle). AP, action potential.

Intracellular coupling during AP-voltage clamping. In cells subjected to AP-voltage clamping, voltage is only unidirectionally coupled to the voltage-dependent components of the cell: voltage influences the voltage-dependent components, but these components cannot influence the clamped voltage. This unidirectional coupling during AP clamping is also depicted in Fig. 1; that is, during AP clamping, voltage (in the form of identical, externally applied AP morphologies) still drives the activity of the cell, but the sarcolemmal currents that are purely voltage dependent [i.e., sodium current (I_{Na}), the rapid component of the delayed rectifier potassium current (I_{Kr}), etc., in Fig. 1] can no longer influence other components of the cell. (For example, a perturbation to I_{Na}, such as an instantaneous change in conductance, will not have a direct effect on the behavior of any other component in the cell during AP-voltage clamping, since membrane voltage, which I_{Na} contributes to in unclamped situations, is clamped to an externally imposed AP morphology.) Unless some of the voltage-dependent components of the cell remain coupled through variables other than voltage [e.g., some intracellular calcium concentration ($[Ca^{2+}]_i$), as occurs with $I_{Ca,L}$ and I_{NaCa}], AP clamping decouples the voltage-dependent components from each other. Given that the purely voltage-dependent components of a cell are constrained to respond to the externally applied period-1 AP morphology alone during AP clamping, non-period-1 rhythms such as calcium alternans [as seen in the AP-voltage clamp experiments described in INTRODUCTION (2, 25)] must arise from the dynamic interaction of those cellular components that remain bidirectionally coupled to each other during AP clamping.

The different coupling arrangements that are present during AP clamping and during pacing suggest that a comparison of the stability (measured as described in *Stability analysis*) of the period-1 rhythm in a paced cell and in an identical but AP-clamped cell will reveal the contribution of bidirectional voltage coupling to the stability of the period-1 rhythm and, hence, to the development of alternans during pacing. Two situations may result from such a comparison: *1*) the stability of the period-1 rhythm of the AP-clamped cell is the same as that of the paced cell; and *2*) the stability is different in each case.

If the stability of the period-1 rhythm of the paced cell is the same as that of the AP-clamped cell, it may be concluded that although those components that are decoupled during AP clamping are necessary for generating the overall AP activity of the cell, they do not directly contribute to modulating the stability of the period-1 rhythm during pacing. In such a situation, only those components of the cell that remain bidirectionally coupled to each other during AP clamping modulate the stability of the period-1 rhythm during pacing. If, on the other hand, the stability of the period-1 rhythm of the AP-clamped cell is different from that of the paced cell, it may be concluded that the components that are decoupled from the rest of the cell during AP clamping play a direct role in dictating the conditions under which alternans occurs.

Downloaded from ajpheart.physiology.org on October 9, 2007

Intracellular coupling during calcium-transient clamping. For this study, we have developed a technique we call "calcium-transient clamping," which is feasible in models but not in experiments. Calcium-transient clamping is directly analogous to AP clamping: during an AP, each calcium concentration within the calcium handling system [e.g., cytoplasmic $[Ca^{2+}]$, sarcoplasmic reticulum (SR) $[Ca^{2+}]$, etc.] is forced to follow its prerecorded period-1 time course, whereas all other components of the cell (including transmembrane voltage) are allowed to run free.

As Fig. 1 indicates, the calcium system (i.e., the intracellular calcium concentrations, uptake and release fluxes in the SR, etc.) of a calcium transient-clamped myocyte is unidirectionally coupled to the calcium-dependent membrane currents of the cell (e.g., $I_{Ca,L}$ and I_{NaCa} in Fig. 1); that is, the calcium system influences these calcium-dependent components, but these components cannot influence the clamped calcium system. The development of non-period-1 rhythms, such as repolarization alternans during calcium-transient clamping, must therefore arise from the dynamic interaction of those cellular components that remain bidirectionally coupled during calcium-transient clamping (i.e., the voltage-dependent sarcolemmal currents).

The unidirectional and bidirectional calcium-dependent coupling that is present during calcium-transient clamping and during pacing, respectively, suggests that a comparison of the stability of the period-1 rhythm in paced and calcium-transient-clamped cells will reveal the role of bidirectional calcium coupling in modulating the stability of the paced period-1 rhythm and, thus, to the development of alternans during pacing.

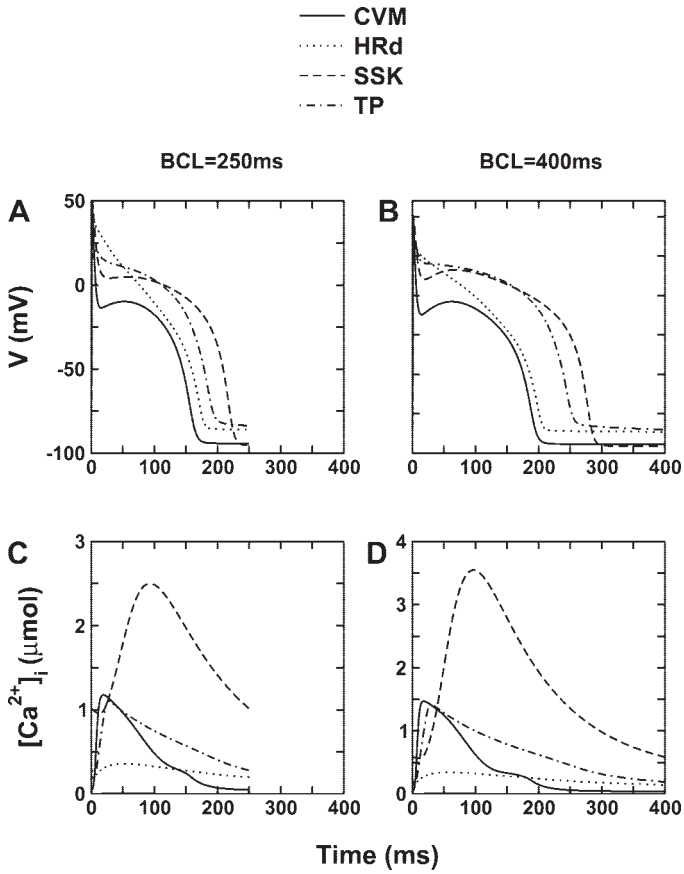

Fig. 2. AP morphologies (*A* and *B*) and intracellular calcium concentration ($[Ca^{2+}]_i$) transients (*C* and *D*) for the 4 models analyzed in this study (see MATERIALS AND METHODS). The models are paced at basic cycle lengths (BCLs) of 250 (*A* and *C*) and 400 ms (*B* and *D*).

MATERIALS AND METHODS

Models. To demonstrate the validity of our approach across a wide range of models and parameter ranges that are frequently used to study alternans and alternans-related phenomena, we studied paced and clamped versions of four ionic models: *1*) the canine ventricular myocyte (CVM) model of Fox et al. (4); *2*) the Hund-Rudy dynamic (HRd) model (11); *3*) the Shiferaw et al. (19) modification of the CVM model, hereafter, the Shiferaw-Sato-Karma (SSK) model (19); and *4*) the ten Tusscher and Panfilov (TP) model (22). APs and $[Ca^{2+}]_i$ transients from each of the four models, obtained at two different cycle lengths, are illustrated in Fig. 2. Unless otherwise noted, all models were implemented exactly as described in their originally published formulations. The use of multiple models allowed us to determine whether the results that we obtain are model specific or are able to be generalized across models. In addition, with the assumption that different types of cells may be better represented by some models rather than others, the use of multiple models allowed us to hypothetically apply our findings to different types of cells and species.

The CVM model (4) is a model of a generic canine ventricular myocyte and includes 13 ionic currents: a fast I_{Na}; an inward rectifier potassium current (I_{K1}); a I_{Ks} and I_{Kr}; a transient outward current (I_{to}); a plateau potassium current (I_{Kp}); a I_{NaK}; a I_{NaCa}; background sodium (I_{Nab}) and calcium (I_{Cab}) currents; a sarcolemmal calcium pump current (I_{pCa}); an L-type calcium current ($I_{Ca,L}$); and a potassium current through the L-type calcium channel (I_{CaK}). The model also incorporates two intracellular calcium concentrations, a cytoplasm concentration ($[Ca^{2+}]_i$) and a SR concentration ($[Ca^{2+}]_{SR}$), with SR release, uptake, and leak fluxes also included.

The HRd model (11) is a recent model of the canine ventricular epicardial AP and intracellular calcium system. It includes 14 sarcolemmal ionic currents [I_{Na}, a slowly inactivating late sodium current ($I_{Na,L}$), $I_{Ca,L}$, I_{NaCa}, I_{pCa}, I_{Cab}, a chloride background current (I_{Clb}), I_{NaK}, I_{Kp}, I_{K1}, I_{Ks}, I_{Kr}, and two I_{to} currents (I_{to1} and I_{to2})]. The model incorporates network and junctional SR; uptake, translocation, release, and leak components of the SR calcium handling system; and four intracellular calcium concentrations: *1*) the calcium concentration in the submembrane space ($[Ca^{2+}]_{ss}$), *2*) the calcium concentration in the bulk cytoplasm ($[Ca^{2+}]_i$), *3*) the calcium concentration in the network SR ($[Ca^{2+}]_{NSR}$), and *4*) the average calcium concentration in the junctional SR ($[Ca^{2+}]_{JSR}$). The model also includes the calcium/calmodulin-dependent protein kinase (CaMKII) regulatory pathway.

The 2006 TP model (22), a modified version of an earlier model (21), was constructed to reproduce the electrophysiological behavior of human epicardial, midmyocardial, and endocardial ventricular myocytes. The model includes 12 ionic currents (I_{Na}, I_{K1}, I_{to}, I_{Kr}, I_{Ks}, $I_{Ca,L}$, I_{NaCa}, I_{NaK}, I_{pCa}, I_{Kp}, I_{Cab}, and I_{Nab}) and three intracellular calcium concentrations [the total cytoplasm $[Ca^{2+}]_i$, the $[Ca^{2+}]_{SR}$, and the subspace concentration ($[Ca^{2+}]_{SS}$)], in addition to release, uptake, and leak currents associated with the SR.

The SSK model (19) is based on many of the same sarcolemmal ion currents as found in the CVM model, with updated calcium-handling system components incorporated from an intracellular calcium cycling model (20) that was originally constructed to shed light on rabbit AP clamp experiments (2). Thus the SSK model cannot be said to readily represent any one particular animal species. The SSK model incorporates formulations of I_{Na}, I_{Kr}, I_{Ks}, I_{Kp}, I_{to}, I_{K1}, $I_{Ca,L}$, and I_{NaCa} and, much like the HRd model, four intracellular calcium concentrations: the calcium concentration in the submembrane space ($[Ca^{2+}]_s$); the calcium concentration in the bulk cytoplasm ($[Ca^{2+}]_i$); the cal-

Downloaded from ajpheart.physiology.org on October 9, 2007

cium concentration in the network SR ($[Ca^{2+}]_j$); and the average calcium concentration in the junctional SR ($[Ca^{2+}]_j'$).

To generate different types of alternans behavior, we have run simulations with the SSK model using different pairs of values of the parameters u (the SR release slope) and τ_f (the time constant of voltage-dependent inactivation of the L-type calcium channel). These are the same parameters as others have altered during previous studies of alternans (19). In all simulations the parameter γ, which regulates the relative contributions of I_{Ca} and I_{NaCa} in the SSK model, was set to 0.7 to produce concordant voltage-calcium alternans (19).

Stability analysis. Alternans arises when the stable period-1 rhythm that is present at slower pacing rates becomes unstable and is replaced by a stable, period-2 (i.e., alternating) rhythm at faster pacing rates. An analysis of the stability of the period-1 rhythm during clamping and during pacing will reveal whether those components that are uncoupled from the rest of the cell during clamping, but remain coupled during pacing, affect alternans onset.

The stability of the period-1 rhythm during alternans may be determined by *1*) locating and controlling the period-1 rhythm using a control algorithm (detailed below in *Obtaining the period-1 rhythm*) and *2*) measuring the rate at which the period-1 rhythm diverges toward the stable, period-2 alternans rhythm when control is released. An example of such a procedure is illustrated in Fig. 3. In Fig. 3*A*, where the AP duration of *beat n* (APD_n) is plotted as a function of beat number, the unstable period-1 rhythm gradually diverges to a stable period-2 rhythm after the control algorithm is turned off. If the rate of divergence is slow, meaning that it takes many beats for the period-2 rhythm to stabilize after control is turned off, the period-1 rhythm is said to be relatively more stable than if the rate of divergence to the period-2 rhythm is rapid.

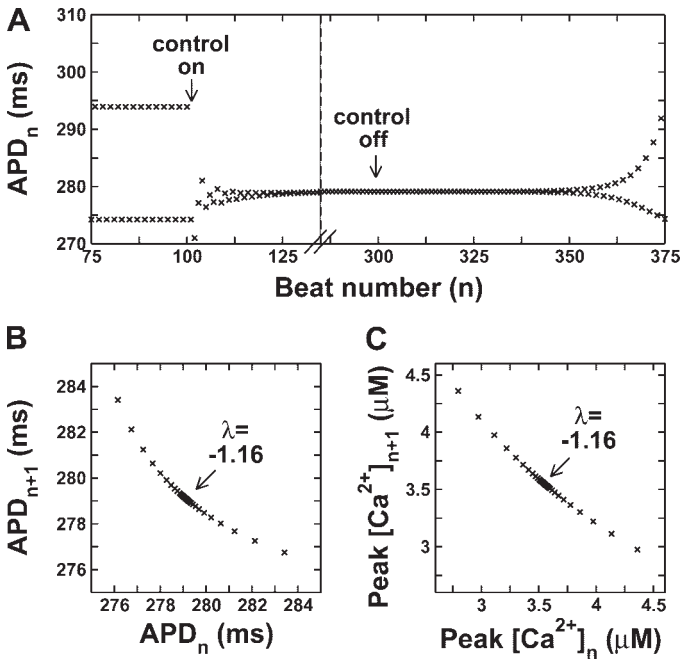

Fig. 3. SSK model cell with parameter values $u = 11.0$ (the sarcoplasmic reticulum release slope), $\tau_f = 60$ ms (the time constant of voltage-dependent inactivation of the L-type calcium channel), and $\gamma = 0.7$ (a parameter that regulates the relative contributions of I_{Ca} and I_{NaCa} in the SSK model). *A*: illustrates how the stable period-2 rhythm during pacing at a cycle length of 400 ms is initially replaced by a period-1 rhythm during control. The unstable period-1 rhythm then diverges to the period-2 rhythm after control is turned off. *B*: plot of the values from *A* on different axes, whereas *C* depicts corresponding peak $[Ca^{2+}]_i$ values. The identical slopes of *B* and *C* (equal to -1.16) around the period-1 fixed point [i.e., where AP duration of *beat n* (APD_n) = APD_{n+1} (*B*), or peak $[Ca^{2+}]_n$ = peak $[Ca^{2+}]_{n+1}$ (*C*)] provide a measure of the stability of the period-1 rhythm.

A plot of APD_{n+1} as a function of APD_n quantifies the rate of divergence to alternans and therefore provides a direct measure of the stability of the period-1 rhythm (9). An example of such a graph, referred to henceforth as a stability curve, is shown in Fig. 3*B*. If the period-1 rhythm is less stable than that shown in Fig. 3, the rate of divergence (depicted in Fig. 3*A*) to stable period-2 alternans will be more rapid and the slope of the stability curve (λ) will be steeper compared with that shown. A plot of peak $[Ca^{2+}]_{n+1}$ as a function of peak $[Ca^{2+}]_n$, as shown in Fig. 3*C*, provides a calcium stability curve that has an identical slope to the APD stability curve in Fig. 3*B*.

Obtaining the period-1 rhythm. For each model cell, brief current injections were given at a constant cycle length to elicit a train of APs. To locate the unstable period-1 rhythm at that cycle length, we applied an alternans control algorithm that perturbed the stimulation interval until the AP rhythm converged to the underlying (unstable) period-1 rhythm (5, 6, 8, 9). Such algorithms are designed to exploit the inherent relationship between APD and preceding diastolic interval by making feedback-controlled perturbations to the diastolic interval that eliminates APD alternans. An example of one such control algorithm is as follows:

$$BCL_n = \begin{cases} BCL^* + \Delta BCL_n & \text{if} \quad \Delta BCL_n < 0 \\ BCL^* & \text{if} \quad \Delta BCL_n \geq 0 \end{cases} \qquad (1)$$

where

$$\Delta BCL_n = (\lambda/2)(APD_n - APD_{n-1}). \qquad (2)$$

Here, BCL_n is the n^{th} basic cycle length (stimulation interval), BCL* is the stimulation interval without control, and (λ/2) is the feedback gain (typically, $\lambda/2 = 0.5$). For this algorithm, small perturbations are made to the stimulation interval (in this case, shortening the interval) until the period-1 rhythm is obtained.

The process of alternans control during pacing is exemplified by the first few beats after control has been turned on in Fig. 3*A*. Once the period-1 rhythm was obtained, the time course of voltage for one full cycle length was recorded, to be used in AP-voltage clamping at a later time. For later calcium-transient clamping, the time courses of all intracellular calcium concentrations [e.g., the four calcium concentrations $[Ca^{2+}]_s$, $[Ca^{2+}]_i$, $[Ca^{2+}]_j$, and $[Ca^{2+}]_j'$ in the SSK model (19)] during one full cycle length were also recorded.

Each model was subjected to pacing, control (to obtain the underlying period-1 rhythm), and subsequent recording of the period-1 time courses of voltage and calcium concentrations over a range of cycle lengths.

Divergence from the period-1 fixed point: pacing. After the unstable period-1 rhythm was obtained at a given cycle length using the control algorithm, the cellular rhythm was allowed to diverge to the stable period-2 alternans rhythm by turning the control algorithm off and continuing to pace the cell at the same fixed interval (as at $n = 300$ in Fig. 3*A*). The durations of each AP and peak $[Ca^{2+}]_i$ during every beat were measured during the divergence process to plot stability curves such as those shown in Fig. 3, *B* and *C*.

Divergence from the period-1 fixed point: AP-voltage clamping. To measure the rate of divergence of the period-1 rhythm during AP-voltage clamping at a given cycle length, we initially applied control to a paced (i.e., unclamped) cell to obtain the period-1 rhythm. We then turned control off and simultaneously began applying the prerecorded AP voltage time course, as a voltage clamp, for one complete cycle length at that pacing rate. The clamp morphology was then applied to all subsequent beats. This meant that the time course of voltage repeated itself in an identical fashion during every subsequent beat, but the intracellular calcium handling system was not clamped in any way and was thus free to develop alternans (as in the experiments conducted in Refs. 2 and 25, as described in INTRODUCTION).

To measure the rate of divergence from the period-1 rhythm during AP clamping, we recorded the peak intracellular calcium concentration from every beat during the divergence to calcium alternans.

Downloaded from ajpheart.physiology.org on October 9, 2007

Plotting the peak $[Ca^{2+}]_i$ of the next beat as a function of the previous beat during AP clamping as the unstable period-1 rhythm diverged to the stable period-2 rhythm resulted in stability curves such as that shown in Fig. 3*C*.

Divergence from the period-1 fixed point: calcium-transient clamping. The rate of divergence of the period-1 rhythm during calcium-transient clamping was measured by first applying control to obtain the unstable period-1 rhythm at a given cycle length. We then turned control off and returned to pacing the cell at the nominal cycle length, while simultaneously applying the prerecorded calcium-transient time course(s) (corresponding to that pacing rate) to the calcium components. Because voltage was not clamped, it was free to develop alternans. The rate of divergence was quantified by measuring the APD of each subsequent beat during the process of divergence.

Confirmation of stability quantification using eigenmode analysis. To confirm the validity of the divergence approach that we used to quantify the stability of the period-1 rhythm during pacing, AP-clamping, and calcium-transient clamping, we also implemented the eigenmode technique of Li and Otani (14) in each scenario. Through perturbation theory, the eigenmode technique separates the various modes (eigenmodes) or behaviors intrinsic to the period-1 rhythm from each other, such that each mode and its contribution to the overall behavior of the period-1 rhythm may be studied in isolation. Eigenmode analysis has previously been used to study the influence of AP morphology on the stability of the period-1 rhythm during AP clamping (13, 19).

The largest negative eigenvalue [referred to as the "alternans eigenvalue" by the developers of the technique (14)] obtained from the eigenmode method quantifies period-1 stability. Given that the alternans eigenvalue and the slope of the stability curve during divergence both measure the rate at which consecutive beats diverge from the unstable period-1 rhythm when alternans behavior dominates, the eigenmode analysis and the divergence technique produced identical quantifications of stability for the models tested here.

We also used the eigenmode approach to quantify the stability of the period-1 rhythm near the transition to alternans (i.e., while it was still stable and therefore not divergent). Thus, for stable period-1 rhythms, the λ values reported in this study were computed using the eigenmode approach. $|\lambda| < 1$ signifies that the period-1 rhythm is stable, whereas $|\lambda| > 1$ signifies an unstable period-1 rhythm.

MODELING RESULTS

SSK model. Figure 4 illustrates the stability characteristics of the SSK model during clamping and pacing. The pairs of values for the parameters u and τ_f shown in Fig. 4 illustrate the rich variety of behaviors that the SSK model can exhibit. More importantly, they demonstrate the ability of our methodology to distinguish between different alternans mechanisms.

In Fig. 4*A*, where the SR release slope (i.e., the steepness of the dependence of SR calcium release on SR load) is steep (i.e., large u) and the voltage-dependent inactivation of $I_{Ca,L}$ is fast (i.e., small τ_f), stability analysis reveals that the AP-clamped (circles) and paced (crosses) cells both exhibit unstable period-1 rhythms across almost the entire range of cycle lengths studied (as indicated by $|\lambda| > 1$ in both cases for all but the longest cycle lengths). For this set of parameter values, the paced cells (i.e., those with bidirectional voltage coupling) possess almost identical stability characteristics to the AP-clamped cells (i.e., those with unidirectional voltage clamping), as indicated by the negligible difference between λ values for these two cases at each cycle length. The calcium transient-clamped cells (triangles), however, are much more stable, as indicated by $|\lambda| \ll 1$ for all but the fastest cycle lengths. Therefore, for the parameter values in Fig. 4*A*, it may be concluded that the voltage-dependent components of the cell (i.e., I_{Na}, I_{Kr}, etc., in Fig. 1) that are coupled to the calcium system through bidirectional voltage coupling during pacing make almost no difference to the stability properties of the paced period-1 rhythm, since the period-1 rhythm possesses the same degree of stability regardless of whether these components are clamped or not. However, the presence of bidirectional calcium coupling is essential for the period-1 rhythm to become unstable, as indicated by the fact that clamping the calcium transients causes the period-1 rhythm to become very stable. Thus, based on the comparison of paced and clamped cells, it may be concluded (for this set of parameter values) that the alternans rhythm is predominantly driven by the dynamics of the calcium system.

In Fig. 4*B*, the voltage-dependent inactivation of $I_{Ca,L}$ has been slowed down (i.e., τ_f is larger), and the SR release slope has been made less steep (i.e., u is smaller) than in Fig. 4*A*. At longer cycle lengths, the paced and AP-clamped cells behave

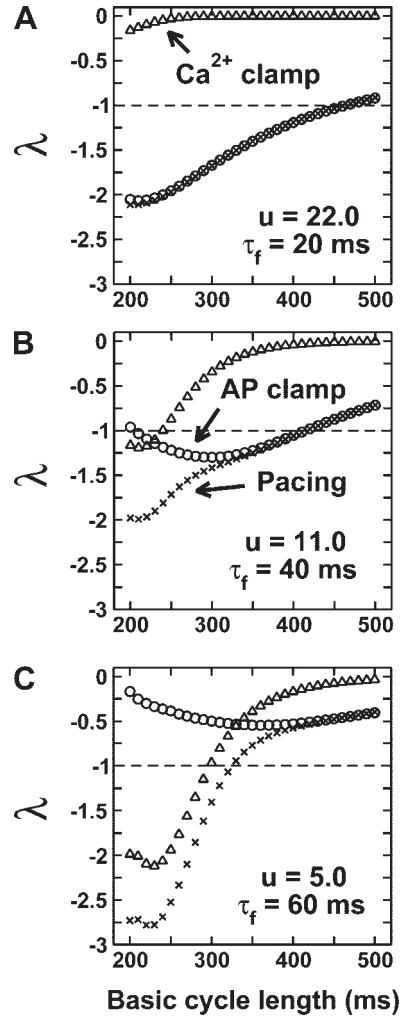

Fig. 4. λ as a function of cycle length for the SSK model during pacing (×), AP clamping (○), and calcium-transient clamping (△). *A–C*: different combination of values of the parameters u and τ_f, as indicated. The bidirectionally coupled (i.e., paced) cells tend to have period-1 rhythms that are less stable than those cells that possess either unidirectional voltage coupling (i.e., AP-clamped cells) or unidirectional calcium coupling (i.e., calcium transient-clamped cells), as indicated by the larger values of $|\lambda|$ during pacing compared with values during clamping.

Downloaded from ajpheart.physiology.org on October 9, 2007

much the same as the cell in Fig. 4*A*; stability analysis reveals that the period-1 rhythms of the AP-clamped and paced cells exhibit almost identical stability properties, whereas the period-1 rhythm of the calcium transient-clamped cell is very stable. However, at shorter cycle lengths, the paced period-1 rhythm is less stable than the period-1 rhythm of the AP-clamped cell, as indicated by the larger $|\lambda|$ values for the paced cell compared with the clamped cells. This difference between λ values for the paced and clamped cells indicates that the presence of bidirectional voltage coupling during pacing tends to make the period-1 rhythm less stable than the period-1 rhythm of the unidirectionally coupled AP-clamped cell; that is, at all but the shortest cycle lengths, the period-1 rhythm of the AP-clamped cell is itself unstable, meaning that the calcium-dependent components that remain coupled during AP clamping are sufficient to generate an unstable period-1 rhythm, but the presence of bidirectional voltage coupling makes the period-1 rhythm more unstable.

Calcium-transient clamping in Fig. 4*B* reveals that bidirectional calcium coupling plays a more prominent role, relative to the contribution of voltage coupling, in regulating the stability of the paced period-1 at rapid pacing rates than at slower pacing rates. At the fastest pacing rates shown, the period-1 rhythm can become unstable even when the calcium transients are clamped. Although this suggests that the interaction of the voltage-dependent components of the cell is sufficient for a non-period-1 rhythm to develop at these pacing rates, the presence of bidirectional calcium coupling causes the paced period-1 rhythm to be significantly less stable (i.e., the paced cell is significantly less stable than the calcium transient-clamped cell). Thus, for this set of parameter values, a comparison of paced and clamped cells reveals that the alternans rhythm is driven by the dynamics of both voltage and the calcium system, with the contribution of each to the overall stability of the system being a function of the cycle length.

Figure 4*C* shows how the clamping and stability analysis techniques reveal the respective roles of bidirectional voltage and calcium coupling as a function of cycle length for yet another set of parameter values in the SSK model. Here, the SR release slope is flatter (i.e., u is smaller) than in Fig. 4, *A* and *B*, making the period-1 rhythm of the AP-clamped cell more stable at every cycle length (as indicated by the overall reduction in $|\lambda|$ for the AP-clamped cell across all cycle lengths). For the values of u and τ_f in Fig. 4*C*, the AP-clamped period-1 rhythm does not become unstable at any cycle length. However, the period-1 rhythm during pacing is significantly less stable than the period-1 rhythm during AP clamping over a wide range of cycle lengths, indicating that in these cells the presence of bidirectional voltage coupling is essential for the paced period-1 rhythm to become unstable.

Whereas the stability of the period-1 rhythm of the AP-clamped cells deviates markedly from that of the paced period-1 rhythm at rapid pacing rates in Fig. 4*C*, the paced and calcium transient-clamped cells exhibit relatively similar stability properties at all pacing rates. This indicates that the calcium-dependent components that are coupled to the voltage system during pacing play a less important role in regulating the stability of the paced period-1 rhythm in these situations, since the period-1 rhythm can become unstable even when these components are clamped. Thus, for this set of parameter values, the alternans rhythm is predominantly driven by the voltage dynamics.

The results in Fig. 4 indicate that the period-1 rhythm of the SSK model becomes unstable over a range of parameter values and pacing rates. The AP and intracellular calcium behavior that is observed when the instability arises, however, is dependent on the particular stimulation protocol that is being applied, as depicted in Fig. 5. In Fig. 5, all results were obtained at a cycle length of 290 ms, with the simulations in Fig. 5, *A–D*, corresponding to the parameter values $u = 11.0$ and $\tau_f = 40$ ms (i.e., Fig. 4*B*), whereas those in Fig. 5, *E* and *F*, correspond to $u = 5.0$ and $\tau_f = 60$ ms (i.e., Fig. 4*C*). In Fig. 5, *A* and *B*, both repolarization and calcium alternans occur during constant pacing. In Fig. 5, *C* and *D*, calcium alternates while transmembrane voltage is repeatedly clamped to the underlying unstable period-1 rhythm. This is similar to experimental observations in rabbit (2) and guinea pig (25) AP-voltage clamping experiments, except that in our simulations, the AP morphology corresponds exactly to the period-1 morphology. In Fig. 5, *E* and *F*, the four intracellular calcium concentration transients in the model were repeatedly clamped to morphologies corresponding to the underlying unstable period-1 rhythm. As a result, the intracellular calcium transient is identical from one beat to the next (Fig. 5*F*), but the AP, which is not clamped in

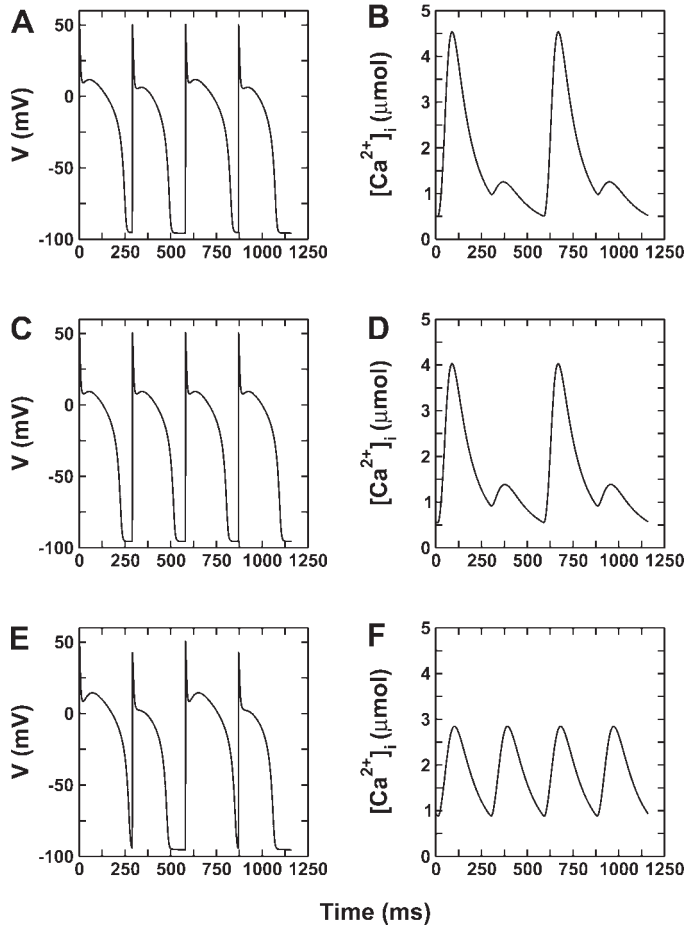

Fig. 5. Membrane potential and $[Ca^{2+}]_i$ behavior during pacing (*A* and *B*), period-1 fixed point AP-voltage clamping (*C* and *D*), and period-1 fixed point calcium-transient clamping (*E* and *F*) at a cycle length of 290 ms in the SSK model. *A–D*: $u = 11.0$ and $\tau_f = 40$ ms. *E* and *F*: $u = 5.0$ and $\tau_f = 60$ ms.

Downloaded from ajpheart.physiology.org on October 9, 2007

any way, exhibits alternans. In this situation (corresponding to Fig. 4*C*), it may be concluded that the alternans rhythm is predominantly driven by the voltage dynamics.

Other models. Similar comparisons of paced, AP-clamped and calcium transient-clamped cells were conducted with three other ionic models, further illustrating the utility of this approach in determining the respective contributions of voltage- and calcium-dependent coupling to alternans. Figure 6 illustrates the results of the stability analysis of the CVM (Fig. 6*A*), HRd (Fig. 6*B*), and TP (Fig. 6*C*) models during pacing, AP clamping, and calcium-transient clamping. Figure 6*C* arises from parameter values in the TP model corresponding to endocardial cells (22). In the CVM model, calcium-transient clamping entailed clamping $[Ca^{2+}]_i$ and $[Ca^{2+}]_{SR}$ (4); in the HRd model, calcium-transient clamping entailed clamping $[Ca^{2+}]_{SS}$, $[Ca^{2+}]_i$, $[Ca^{2+}]_{JSR}$, and $[Ca^{2+}]_{NSR}$ (11); whereas in the TP model, calcium-transient clamping was applied by clamping $[Ca^{2+}]_i$, $[Ca^{2+}]_{SR}$, and $[Ca^{2+}]_{SS}$ (22).

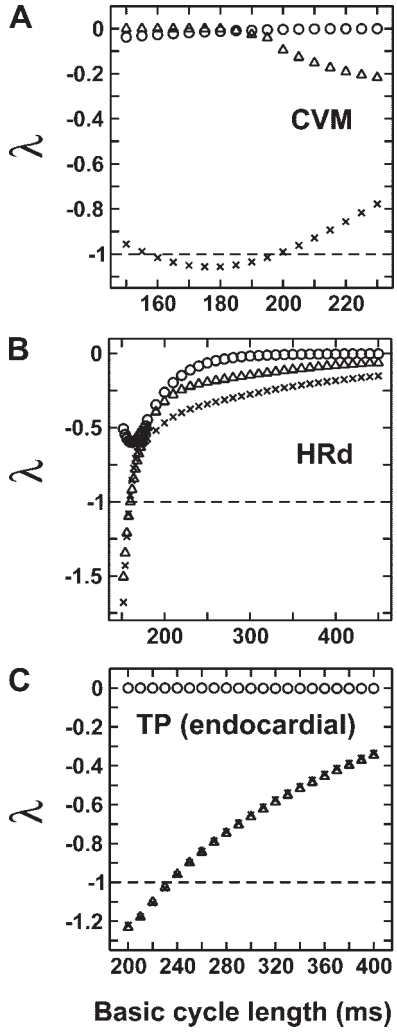

Fig. 6. λ as a function of cycle length for the CVM (*A*), HRd (*B*), and TP (*C*) models during pacing (×), AP clamping (○), and calcium-transient clamping (△). Parameter values for the TP model were selected to correspond to human endocardial cells, with intracellular sodium concentration and intracellular potassium concentration kept constant. As for the SSK model, the period-1 rhythm of each cell tends to be less stable in the presence of bidirectional voltage coupling (i.e., during pacing) compared with unidirectional voltage coupling (i.e., during AP clamping), as indicated by the larger values of $|\lambda|$ during pacing compared with during AP clamping. The presence of bidirectional calcium coupling during pacing has model-dependent effects on the period-1 rhythm.

For the CVM model (Fig. 6*A*), clamping either voltage or the intracellular calcium transients makes the period-1 rhythm much more stable compared with the period-1 rhythm during pacing. Indeed, as Fig. 6*A* suggests, both bidirectional calcium and voltage coupling must be present for the paced period-1 rhythm of the CVM model to become unstable, since neither the voltage- nor the calcium transient-clamped cells exhibit unstable period-1 rhythms.

Similarly, the period-1 rhythm of the AP-clamped HRd model (Fig. 6*B*) is more stable than the period-1 rhythm during pacing across the entire range of pacing rates studied. Calcium-transient clamping applied to the HRd model reveals that the period-1 rhythms of the calcium transient-clamped and paced cells exhibit very similar stability properties, although the presence of bidirectional calcium coupling tends to have a slightly destabilizing effect on the paced period-1 rhythm (as indicated by the fact that the period-1 rhythm of the calcium transient-clamped cell is slightly more stable than the period-1 rhythm of the paced cell across almost all of the pacing rates studied).

For the TP model (Fig. 6*C*), values from simulated epicardial and midmyocardial cells are not shown, since simulations of these cells resulted in stability characteristics that were qualitatively similar to that of endocardial cells. In all three cases in the TP model, the period-1 rhythm during AP clamping was much more stable than the period-1 rhythm during pacing, indicating that bidirectional voltage coupling plays an important role in regulating the stability of the paced period-1 rhythm. As Fig. 6*C* indicates, the period-1 rhythm of the calcium transient-clamped cell exhibits practically identical stability properties to the period-1 rhythm of the paced cell, indicating that the presence of bidirectional calcium coupling tends to have practically no effect on the stability of the paced period-1 rhythm. These results can be contrasted with Fig. 4*A*, where for those parameter values in the SSK model, the presence of bidirectional voltage coupling tended to have practically no effect on the stability of the paced period-1 rhythm.

It should be noted that, in Figs. 4 and 6, the pacing rates at which alternans is initiated (i.e., when $|\lambda| = 1$) in each model and the range of pacing rates over which each model exhibits alternans (i.e., when $|\lambda| > 1$) are different. Given that each model was created to reproduce the behavior of different kinds of cells and that the models possess varying degrees of complexity, these differences are not surprising. It must be emphasized that the pacing rates at which alternans occurs are not important for this study; what is important is the fact that our methodology can characterize the contributions of voltage- and calcium-dependent coupling to the stability of the period-1 rhythm in any ionic model, as the results in these two figures indicate.

DISCUSSION OF MODELING RESULTS

A growing body of experimental evidence appears to support the hypothesis that intracellular calcium cycling alternans is the primary cause of repolarization alternans. A number of experimental studies have been conducted that provide support

Downloaded from ajpheart.physiology.org on October 9, 2007

for this hypothesis (2, 3, 7, 10, 12, 15, 24, 25); a great deal of this evidence has been discussed extensively in a recent review article (23). Although it has been suggested that the electrical system plays more than a follower role, even when calcium may be the primary driver of alternans (13, 19), the significance of this role has remained unclear. In the present study, we show that by directly comparing clamped and paced cells, it is possible to determine the contributions of voltage- and calcium-dependent coupling to the stability of the period-1 rhythm during pacing.

In the process of demonstrating the utility of this method, we found that, for some model types or parameter regimes, the presence of bidirectional voltage coupling had little to no effect on the stability of the period-1 rhythm, indicating that in such situations the stability of the period-1 rhythm is predominantly regulated by calcium. In other cells, bidirectional voltage coupling did contribute to the instability of the period-1 rhythm; these contributions ranged from minor to being necessary for the period 1 to become unstable. In such cells, alternans is actually caused by a combination of mechanisms (*I*) and (*II*) (as defined in INTRODUCTION).

A complementary comparison of calcium transient-clamped and paced cells similarly revealed the role of bidirectional calcium coupling in regulating the stability of the period-1 rhythm during pacing. Like bidirectional voltage coupling, the presence of bidirectional calcium coupling tended to destabilize the period-1 rhythm, with the degree of destabilization dependent on the particular model type or parameter regime being studied.

What are we to make of this broad range of results? Their importance lies not in the fact that different models exhibit different relative contributions from bidirectional voltage- and calcium-dependent coupling to their mechanisms of repolarization alternans; this outcome could perhaps have been predicted simply by perusing the disparate mathematical formulations of the models studied. What is important is that this study demonstrates for the first time that a combination of clamping and stability analysis can quantify the relative contributions of calcium and voltage dynamics to repolarization alternans, thereby pointing toward a solution of the "chicken and egg" problem of understanding the cause of repolarization alternans in any model cell.

Which model is best for studying alternans? The results of the simulations conducted in this study reveal that different models exhibit different relative contributions from bidirectional voltage- and calcium-dependent coupling to the mechanism of repolarization alternans. As the discussion of the models in MATERIALS AND METHODS revealed, the models studied here possess a variety of formulations and degrees of complexity, both with regard to voltage dynamics and intracellular calcium handling, with the most recent models possessing more detailed calcium handling systems than earlier models. Given the diversity of model formulations, it is not particularly surprising to find that the instability in the period-1 rhythm that leads to alternans in some cases is driven predominantly by calcium system dynamics; in others, predominantly by the voltage dynamics; and in yet others, by some combination of the two.

Although the differences between models are striking, we do not believe that it is possible, nor indeed helpful, to postulate which of these models best reproduces the alternans dynamics of real cardiac myocytes. This is so for (at least) two reasons. First, because the alternans mechanism in different cell types or species may be qualitatively different (17, 18), or because particular models may only be valid under certain conditions, more than one of the models may be accurate in reproducing the alternans dynamics found in real myocytes. Second, as we explain in PROPOSED EXPERIMENTAL STUDIES, we believe that the necessary experiments for teasing apart the relative contributions of the voltage and calcium system dynamics to alternans have not yet been conducted. As described in the INTRODUCTION, experimental studies have produced results that are inconclusive as to the mechanism of repolarization alternans in real myocytes.

Comparison with previous modeling studies. The contribution of the coupling between cellular components to alternans has received limited attention to date. A recent modeling study investigated aspects of the coupling between calcium and voltage during alternans in an ionic model, focusing particularly on the types of AP behavior that emerge from positive coupling (leading to concordant electromechanical alternans) and from negative coupling (leading to discordant electromechanical alternans) between these two systems during pacing (19). In addition to the results obtained from the ionic model, a simplified low-dimensional map model was derived and used to analytically uncouple voltage and calcium to determine their respective contributions to stability. A linear stability analysis of this map model revealed that the stability of the period-1 rhythm was governed by the stability of the voltage system, the stability of the calcium system, and the coupling between these two systems. Analytical predictions of the stability of the period-1 rhythm were obtained in terms of the stability of each of these three parts of the cell, thereby revealing the relative contribution of each part to the stability of the period-1 rhythm for that model (19).

The present study has sought to achieve a similar goal of uncoupling the cellular components that are believed to play important roles in alternans, but with full ionic models rather than with a simplified low-dimensional map model. Because the stability of the period-1 rhythm of the ionic models that we studied here cannot be obtained analytically, we have used voltage and calcium-transient clamping to approximately determine the relative contributions of voltage- and calcium-dependent coupling to alternans.

It should also be noted that, in the map model study of Ref. 19, the linear stability analysis of the map model resulted in the voltage and calcium systems being completely isolated from each other. In real myocytes, these two systems are never completely isolated from each other; for example, the calcium system requires the influx of calcium through the L-type calcium channels during the AP to initiate calcium-induced calcium release from the SR, and the current passing through the sodium-calcium exchanger influences the morphology of the AP. By using AP and calcium-transient clamping, we sought to isolate the behavior of the voltage and calcium systems as fully as possible by controlling the nature of the coupling between these two systems. The advantage of this approach over the map model approach is that it can be used to study any ionic model. Furthermore, as we describe in PROPOSED EXPERIMENTAL STUDIES, the AP clamping stability analysis can also be performed experimentally.

Downloaded from ajpheart.physiology.org on October 9, 2007

The selection of proper clamping morphologies is vital for correctly probing the stability of the period-1 rhythm. In the case of AP clamping, the fact that $I_{Ca,L}$ and I_{NaCa} are sensitive to voltage as well as to calcium means that even though these currents are free to interact with (and be influenced by) the other calcium-sensitive components of the cell, the behavior of these two currents will always be partly constrained by the particular AP morphology that is applied to the cell. Therefore, different AP morphologies will force these currents to behave differently and will thereby alter the interaction between these currents and the calcium handling system, causing the period-1 rhythm to exhibit different stability properties for different AP morphologies (as was shown in Ref. 13). Thus the use of an AP morphology other than the real period 1 (necessarily obtained using a control method as in this study) cannot correctly probe the stability of the period-1 rhythm and therefore cannot be used to conclusively illuminate the mechanism of alternans.

PROPOSED EXPERIMENTAL STUDIES

The results of this study suggest that a series of experiments comparing clamped and unclamped myocytes could help to determine the importance of voltage- and calcium-dependent coupling in the development of instabilities in the period-1 rhythm leading to alternans in real cardiac myocytes. Although it is not possible in experiments to conduct calcium-transient clamping as was developed and used in this study, our simulation results suggest that a direct comparison of paced and AP-clamped cells will reveal a great deal about the importance of bidirectional voltage coupling in the development of instabilities such as alternans.

Our proposed experiments are similar in some ways to experiments described in Refs. 2 and 25. In those experiments, $[Ca^{2+}]_i$ in isolated ventricular myocytes was imaged during both pacing and AP clamping. Calcium alternans during AP clamping was observed in both studies, leading to the correct conclusion that, for AP-clamped cells, "any beat-to-beat alterations in the intracellular calcium transient must be an inherent property of intracellular calcium dynamics, and not secondary to alterations in the AP" (2).

As we mention in the INTRODUCTION, however, such a conclusion cannot necessarily be extended to unclamped cells; this can be seen by considering such experimental AP-clamping results in light of the simulation results in Fig. 4 of the present study. Cells characterized, for instance, by the stability characteristics in Fig. 4, *A* and *B*, possess a region where the paced and AP-clamped cells both exhibit stable period-1 rhythms (indicated by $|\lambda| < 1$) at slower pacing rates and a region where the paced and AP-clamped cells both exhibit unstable period-1 rhythms (indicated by $|\lambda| > 1$) at faster pacing rates (a fact that would be manifested in an experiment as a higher-order rhythm such as calcium alternans). From the simple observation as to whether or not alternans occurred (as in Refs. 2 and 25), it is not possible to determine whether the period-1 rhythm of the paced cell exhibits the same stability properties as the period-1 rhythm of the AP-clamped cell (corresponding to a scenario depicted in Fig. 4*A*) or whether the period-1 rhythm of the paced cell is significantly less stable than the period-1 rhythm in the AP-clamped cell (corresponding to a large region of Fig. 4*B*); that is, we have no way to tell from standard AP-clamping experiments (as in Refs. 2 and 25) whether bidirectional voltage coupling plays a significant role in the development of repolarization alternans in the cell (as it does in a cell like that shown in Fig. 4*B*) or whether it plays little to no role at all (as in Fig. 4*A*).

We believe that it is possible to discriminate between such different cell types (and different alternans mechanisms) by performing experimental versions of the simulations conducted in this study over a range of cycle lengths during alternans, using the same general procedure that we described in MATERIALS AND METHODS. Individual cells would be subjected to pacing and AP-clamping, with divergence from the period-1 rhythm during clamping measured by imaging intracellular calcium. The stability of the period-1 calcium rhythm would then be obtained from the slopes of the resulting stability curves. A comparison of the slopes of the stability curves would reveal whether bidirectional voltage coupling plays a role in modulating the stability of the period-1 calcium rhythm of the cell. Such direct insights into the role of voltage coupling in alternans have not been obtained using past experimental methodologies.

It is important to note that the control algorithms used in this study have been demonstrated experimentally to be very robust (for systems that are not spatially extended, such as single cells) (1, 8). Such experimental results indicate that the control approach proposed here is feasible.

AP morphology during clamping. For the proposed experimental stability quantification to be valid, it is necessary that the real period-1 AP morphology be used for AP clamping (as discussed in DISCUSSION). That being said, further investigations are needed to systematically determine the degree of sensitivity of the calcium-handling system stability quantification to AP morphology in experiments; i.e., how exact must the period-1 morphology be to provide a reasonable estimate of the stability?

Limitations of proposed experiments. The proposed experiments rely on the ability to distinguish between the slopes of curves whose data points will most likely be obtained using calcium imaging techniques (as in Ref. 2). If the experimental data are too noisy, it is likely to be difficult, if not impossible, to distinguish between the slopes of these curves. However, this is a potential, practical, rather than theoretical, limitation of our proposed experiments.

GRANTS

This research was supported by National Science Foundation Grant PHY-0513389 and the Kenny Gordon Foundation. P. N. Jordan was also supported by a predoctoral fellowship from the Howard Hughes Medical Institute.

REFERENCES

1. **Christini DJ, Riccio ML, Culianu CA, Fox JJ, Karma A, Gilmour RF Jr.** Control of electrical alternans in canine cardiac purkinje fibers. *Phys Rev Lett* 96: 104101, 2006.
2. **Chudin E, Goldhaber J, Garfinkel A, Weiss J, Kogan B.** Intracellular Ca^{2+} dynamics and the stability of ventricular tachycardia. *Biophys J* 77: 2930–2941, 1999.
3. **Diaz ME, O'Neill SC, Eisner DA.** Sarcoplasmic reticulum calcium content fluctuation is the key to cardiac alternans. *Circ Res* 94: 650–656, 2004.
4. **Fox JJ, McHarg JL, Gilmour RF Jr.** Ionic mechanism of electrical alternans. *Am J Physiol Heart Circ Physiol* 282: H516–H530, 2002.
5. **Gauthier DJ, Bahar S, Hall GM.** Controlling the dynamics of cardiac muscle using small electrical stimuli. In: *Neuro-Informatics and Neural*

Downloaded from ajpheart.physiology.org on October 9, 2007

Modelling, edited by Moss F, and Gielen S. Amsterdam, The Netherlands: Elsevier Science, 2001, p. 229–255.
6. **Gauthier DJ, Socolar JES.** Dynamic control of cardiac alternans—comment. *Phys Rev Lett* 79: 4938, 1997.
7. **Goldhaber JI, Xie LH, Duong T, Motter C, Khuu K, Weiss JN.** Action potential duration restitution and alternans in rabbit ventricular myocytes: the key role of intracellular calcium cycling. *Circ Res* 96: 459–466, 2005.
8. **Hall GM, Gauthier DJ.** Experimental control of cardiac muscle alternans. *Phys Rev Lett* 88: 198102, 2002.
9. **Hall K, Christini DJ, Tremblay M, Collins JJ, Glass L, Billette J.** Dynamic control of cardiac alternans. *Phys Rev Lett* 78: 4518–4521, 1997.
10. **Hirayama Y, Saitoh H, Atarashi H, Hayakawa H.** Electrical and mechanical alternans in canine myocardium in vivo. Dependence on intracellular calcium cycling. *Circulation* 88: 2894–2902, 1993.
11. **Hund TJ, Rudy Y.** Rate dependence and regulation of action potential and calcium transient in a canine cardiac ventricular cell model. *Circulation* 110: 3168–3174, 2004.
12. **Huser J, Wang YG, Sheehan KA, Cifuentes F, Lipsius SL, Blatter LA.** Functional coupling between glycolysis and excitation-contraction coupling underlies alternans in cat heart cells. *J Physiol* 524: 795–806, 2000.
13. **Jordan PN, Christini DJ.** Action potential morphology influences intracellular calcium handling stability and the occurrence of alternans. *Biophys J* 90: 672–680, 2006.
14. **Li M, Otani NF.** Ion channel basis for alternans and memory in cardiac myocytes. *Ann Biomed Eng* 31: 1213–1230, 2003.
15. **Pruvot EJ, Katra RP, Rosenbaum DS, Laurita KR.** Role of calcium cycling versus restitution in the mechanism of repolarization alternans. *Circ Res* 94: 1083–1090, 2004.
16. **Roden DM, Balser JR, George AL Jr, Anderson ME.** Cardiac ion channels. *Annu Rev Physiol* 64: 431–475, 2002.
17. **Saitoh H, Bailey JC, Surawicz B.** Alternans of action potential duration after abrupt shortening of cycle length: differences between dog Purkinje and ventricular muscle fibers. *Circ Res* 62: 1027–1040, 1988.
18. **Saitoh H, Bailey JC, Surawicz B.** Action potential duration alternans in dog Purkinje and ventricular muscle fibers. Further evidence in support of two different mechanisms. *Circulation* 80: 1421–1431, 1989.
19. **Shiferaw Y, Sato D, Karma A.** Coupled dynamics of voltage and calcium in paced cardiac cells. *Phys Rev E Stat Nonlin Soft Matter Phys* 71: 021903, 2005.
20. **Shiferaw Y, Watanabe MA, Garfinkel A, Weiss JN, Karma A.** Model of intracellular calcium cycling in ventricular myocytes. *Biophys J* 85: 3666–3686, 2003.
21. **Ten Tusscher KH, Noble D, Noble PJ, Panfilov AV.** A model for human ventricular tissue. *Am J Physiol Heart Circ Physiol* 286: H1573–H1589, 2004.
22. **Ten Tusscher KH, Panfilov AV.** Alternans and spiral breakup in a human ventricular tissue model. *Am J Physiol Heart Circ Physiol* 291: H1088–H1100, 2006.
23. **Walker ML, Rosenbaum DS.** Repolarization alternans: implications for the mechanism and prevention of sudden cardiac death. *Cardiovasc Res* 57: 599–614, 2003.
24. **Walker ML, Wan X, Kirsch GE, Rosenbaum DS.** Hysteresis effect implicates calcium cycling as a mechanism of repolarization alternans. *Circulation* 108: 2704–2709, 2003.
25. **Wan X, Laurita KR, Pruvot EJ, Rosenbaum DS.** Molecular correlates of repolarization alternans in cardiac myocytes. *J Mol Cell Cardiol* 39: 419–428, 2005.

Downloaded from ajpheart.physiology.org on October 9, 2007